Antibacterial effects of carbon quantum dots@hematite nanostructures deposited on titanium against Gram-positive and Gram-negative bacteria

Omran Moradlou*, Zeinab Rabiei, Niusha Delavari

Department of Chemistry, Alzahra University, P.O. Box: 1993893973, Tehran, Iran.

E-mail: moradlou@alzahra.ac.ir

Abstract

Thin films of nanostructured hematite (α-Fe_2O_3) and carbon quantum dots-incorporated hematite (CQDs@α-Fe_2O_3) were uniformly grown on titanium substrate and their antibacterial properties against Gram-positive (*S. aureus*) and Gram-negative (*E. coli*) bacteria were studied under dark and illumination conditions. The surface morphology of the samples was investigated with FE-SEM and HRTEM. The antimicrobial investigations demonstrate that α-Fe_2O_3 and CQDs@α-Fe_2O_3 are toxic to the selected microorganisms and the samples exhibit sustainable antibacterial activity against Gram-positive bacterial strains compared to Gram-negative bacteria mainly due to the presence of extra outer membrane layer in Gram negative bacteria. Based on the results of the antibacterial activity of α-Fe_2O_3 and CQDs@α-Fe_2O_3 under dark and the light irradiation conditions, it was concluded that the preferred mechanism of bactericidal activity of hematite-based thin films is both the penetration of iron cations into the bacteria cell via their membrane and the generation of reactive oxygen species. These results indicate that CQDs@α-Fe_2O_3 nanoparticulates provide insight into the development of visible-light antimicrobial materials for their potential bactericidal applications.

Keywords: Titanium, Hematite; carbon quantum dots; antibacterial activity; thin film,

1. Introduction

Increasing bacterial resistance through evolutionary processes towards conventional antibiotics such as penicillin and amoxicillin is a major global health concern in current era [1,2]. These antibiotics are chemically modified natural compounds including β-lactams and are the backbone to combat contagious diseases. Although these antibiotics have transformed modern medicine and saved millions of lives [2], however, the broad use and abuse have resulted in emergence of bacterial resistance and adverse side effects [3]. So, the treatment of bacterial infections utilizing these classical antibiotics is certainly becoming more serious global problem [1,4].

In this regard, among all the new developed strategies, the use of nanostructured metal oxides can be emerged as a promising alternative with very distinct pathways of bactericidal action [5-8]. In fact, owing to their multiple mechanisms of bactericidal action, metal oxides would serve as a new class of effective disinfectants with different mechanism compared to the conventional antibiotics. In addition, besides to their use as antimicrobial compounds, they may have diverse applications in food packaging as well as the coating agents on medical devices and implants to make them resistant against microbial infections [3]. Titanium-based alloys are biocompatible and are finding ever-increasing applications as biomaterials in orthopedic implant materials and devices due to their excellent mechanical and biological performance [9].

The mechanism of the bacteria killing under the irradiation of semiconductor-based materials is mainly the photogeneration of electron-hole (e^--h^+) pairs at the surface of illuminated sample. The electrons in the conduction band of the semiconductor can react with molecular oxygen and produce superoxide anion ($O_2^{\bullet-}$) through a reductive process, and holes in the valence band can oxidize water to generate reactive hydroxyl radicals ($^{\bullet}OH$) [23]. However, the disadvantage of using TiO_2 and ZnO is their wide bandgap that UV light is required to activate the photocatalyst and initiate the killing of the bacteria. So, from this point of view, the investigation of the antibacterial activity of the visible light active materials such as hematite is important.

Among the semiconducting metal oxides, iron oxides including hematite (α-Fe_2O_3) [3,27-30], maghemite (γ-Fe_2O_3) [31] and magnetite (Fe_3O_4) [27] exhibit efficient bactericidal properties over a wide spectrum of bacteria. Interestingly, iron oxide-based compounds are biocompatible and have minimal or no cytotoxicity to human cells [3,32,33]. So, they can locally kill bacteria or slow down their growth, without being in general toxic to surrounding tissue. Although the antibacterial activity of maghemite and magnetite have been widely studied, the bactericidal

action of hematite is still under investigation. Interestingly, it was reported that hematite is non-toxic to beneficial soil microbes and does not cause lysis of red blood cells [36]. Finally, hematite have already been approved by the Food and Drug Administration (FDA) for food and medical applications [3,27,28]. So, it seems that there is still a sustained interest in the development of antibacterial activity of hematite-based materials under dark and the illumination conditions.

In this work, regarding the above-mentioned issues on α-Fe_2O_3 and CQDs and based on our recent works on quantum sized carbon materials and the interesting results in photocatalytic and photoelectrochemical processes [35] as well as Fenton-like reactions [45], we selected CQDs to examine the antibacterial activity of CQDs@α-Fe_2O_3. So, the bactericidal properties of hematite (α-Fe_2O_3) and carbon quantum dots-incorporated hematite (CQDs@α-Fe_2O_3) against Gram-positive (*S. aureus*) and Gram-negative (*E. coli*) bacteria are studied under dark and illumination conditions. Based on the obtained results, Ti/α-Fe_2O_3 and Ti/CQDs@α-Fe_2O_3 samples exhibit sustainable antibacterial activity against *S. aureus* strains compared to *E. coli*. So, it is expected that the hematite-based nanomaterials may provide insight into the development of visible-light antimicrobial materials for their potential applications in medical devices.

Experimental

Fabrication of Ti/α-Fe_2O_3 and Ti/CQD@α-Fe_2O_3

For the synthesis of carbon quantum dots (CQDs), an electrochemical method was used as reported elsewhere [46] by using two graphite rods as anode and cathode. Briefly, the graphite electrodes were immersed in a 100 ml solution of ethanol:H_2O (99:1) containing 0.30 g of sodium hydroxide (NaOH), and a constant current intensity of 180 mA cm^{-2} was applied for 24 h. The obtained soluble CQDs were then separated by silica-gel column chromatography after the treatment with $MgSO_4$ [46].

Ti/α-Fe_2O_3 and Ti/CQD@α-Fe_2O_3 samples were fabricated by the hydrothermal method as reported in our previous work [35].

Antibacterial test

The antibacterial activities of the Ti/α-Fe_2O_3 and Ti/CQD@α-Fe_2O_3 samples against Gram-positive *Staphylococcus aureus* (*S. aureus*, ATCC 6538, PTCC 1112) and Gram-negative

Escherichia coli (*E. coli*, ATCC 25922, PTCC 1399) bacteria were studied under dark and illumination conditions by using an antibacterial drop test. 100 µL of saline solution containing bacteria was spread on the surface of each sample in a sterilized Petri dish in incubator. After 24 h, the bacteria were transferred to a nutrient agar plate and incubated at 37 ºC for 24 h for counting the surviving bacterial colonies using an optical microscope. The tests were also examined under the illumination conditions. After the spread of saline solution containing bacteria on the surface of sample, the sample was irradiated by a 30 mW cm^{-2} tungsten lamp at room temperature in incubator. Finally, after 24 h light irradiation, the bacteria were transferred to a phosphate buffer saline solution and the bacterial suspension was spread on a nutrient agar plate and incubated at 37 ºC for 24 h for counting the surviving bacterial colonies. The reported data were the mean values of three distinct experiments. The uncoated Ti sheet was used as a control sample in all the antibacterial tests.

3. Results and discussion

Sample characterization

Fig. 1 a and b show the FE-SEM images of α-Fe_2O_3 and CQD@α-Fe_2O_3 deposited on Ti substrate, respectively. As we have reported recently in our previous work [35], in the synthesis of CQD@α-Fe_2O_3 nanoparticles, CQDs act as nano-scaffolds for the growth of CQD@α-Fe_2O_3 nanoparticulates as core@shell nanostructures.

Bactericidal effects of samples against *S. aureus* and *E. coli* under dark conditions

The bactericidal activity of the prepared Ti/α-Fe_2O_3 and Ti/CQD@α-Fe_2O_3 samples was assessed against two pathogenic bacterial strains including *S. aureus* and *E. coli* under dark conditions. As **Fig. 2** and **Table 1** shows, the bactericidal activity of Ti/α-Fe_2O_3 against *E. coli* was low (~10%). In contrast, about 65% of the *S. aureus* bacteria was inactivated by Ti/α-Fe_2O_3 sample. By using Ti/CQD@α-Fe_2O_3 sample, about 20% of *E. coli* and 70% of *S. aureus* bacteria were inactivated under dark conditions. The higher resistance of Gram negative strain against hematite-based compounds and more antibacterial activity of the samples against Gram positive bacterial strains is mainly due to the presence of extra outer membrane layer in Gram negative bacteria [27]. So, hematite has more prominent toxicity against Gram positive bacterial strains and the Gram negative strain has higher resistance against hematite.

Fig. 1

The antibacterial activity of Ti/α-Fe_2O_3 and Ti/CQD@α-Fe_2O_3 samples against bacterial strain in dark conditions can be assigned to the release of Fe^{3+} ions from α-Fe_2O_3 or CQD@α-Fe_2O_3 and their interaction with cytoplasmic water inside bacterial cell (called Fenton reaction) and then, the formation of reactive oxygen species (ROS) such as superoxide $O_2^{\bullet-}$ and hydroxyl ($^{\bullet}OH$) radicals [3,47]. ROS can penetrate to the cell membrane of bacteria and damage their proteins and DNA, and ultimately results in death of bacteria [48,49]. Fig. 3 shows the zone of inhibition produced by samples Ti/α-Fe_2O_3 and Ti/CQD@α-Fe_2O_3 against *E. coli* and *S. aureus* bacterial strains.

Fig. 2, Fig. 3

Photoinactivation of ***E. coli*** **and** ***S. aureus***

Because the energy band gap of both samples is ~2.1 eV [35], they were illuminated by a tungsten lamp as visible light source. When the samples are illuminated, the electron-hole pairs (e^--h^+) are generated at the surface of semiconductor. So, the electrons with high reducing power in the conduction band can react with molecular oxygen to produce reactive superoxide anion radicals ($O_2^{\bullet-}$), and the holes in the valence band of semiconductor can abstract electrons from water to generate reactive hydroxyl radicals ($^{\bullet}OH$) through an oxidative process [25]. In fact, under the light illumination, it is expected that the higher amounts of ROS would be generated and consequently, lower percent of the bacteria would be survived. The results (**Fig. 4** and **Table 1**) showed that the inactivation of *E. coli* with Ti/α-Fe_2O_3 under the light illumination is about 50% higher than over dark conditions. Also, the photoinactivation of *E. coli* with Ti/CQD@α-Fe_2O_3 sample under the light illumination is higher compared to dark conditions (Table 1) most likely due to the generated e^--h^+ pairs on Ti/CQD@α-Fe_2O_3, resulting more generated ROS on Ti/CQD@α-Fe_2O_3 sample.

Fig. 4

Table 1. Antibacterial activity results of Ti/α-Fe_2O_3 and Ti/CQD@α-Fe_2O_3 samples under dark and visible light illumination conditions

Condition	Microorganism	Initial concentration (CFU/mL)	Sample	Antibacterial activity (%)
Dark	*E. coli*	1.3×10^6	Ti/α-Fe_2O_3	10
		1.2×10^6	Ti/CQD@α-Fe_2O_3	20
	S. aureus	4.1×10^5	Ti/α-Fe_2O_3	65
		7.1×10^5	Ti/CQD@α-Fe_2O_3	70
Visible light illumination	*E. coli*	1.3×10^6	Ti/α-Fe_2O_3	15
		1.0×10^6	Ti/CQD@α-Fe_2O_3	35
	S. aureus	5.3×10^5	Ti/α-Fe_2O_3	70
		3.3×10^5	Ti/CQD@α-Fe_2O_3	80

As we reported recently in our previous work [35], under the light illumination, CQDs as conductive nano-scaffold have the pivotal role in CQD@α-Fe_2O_3 to overcome the short hole-diffusion length and poor hole mobility limitations of hematite. So, higher amounts of holes can diffuse toward the surface of Ti/CQD@α-Fe_2O_3 sample and consequently, higher amounts of reactive $^{\bullet}OH$ radicals will be produced at the surface of Ti/CQD@α-Fe_2O_3 sample. In fact, based on these studies, the probable mechanism is the h^+ transfer (or h^+ hopping) from valence band (VB) of α-Fe_2O_3 to the HOMO of CQDs. **Fig. 5** shows the bacteria inactivation kinetics by Ti/CQD@α-Fe_2O_3 sample under visible light irradiation.

Fig. 5

The FE-SEM images of native and treated *S. aureus* and *E. coli* bacteria strains with Ti/CQD@α-Fe_2O_3 sample are shown in **Fig. 6**. The iron cations can penetrate into the bacteria cell via their membrane. So, it can be concluded that the prevailing mechanism is the diffusion of Fe^{3+} ions inside the bacteria and producing ROS radicals.

Fig. 6

To investigate the stability of Ti/CQD@α-Fe_2O_3 samples in antibacterial tests, the experiments were performed for three cycles. Based on the obtained results, *E. coli* and *S. aureus* were inactivated 31±6% and 78±5%, respectively, indicating that the sample had almost its

bactericidal activity and the bacterial inactivation kinetics are not slow down. These obtained results indicate that the fabricated samples are promising candidates for antibacterial applications in food packaging and orthopedic implants.

4. Conclusions

Herein, thin films of hematite and carbon quantum dots-incorporated hematite were tightly deposited on titanium substrate and their antibacterial properties against *S. aureus* and *E. coli* bacteria were studied under dark and illumination conditions. The obtained results demonstrate that CQDs@α-Fe_2O_3 exhibit sustainable antibacterial activity against *S. aureus* bacterial strains compared to *E. coli* mainly due to the presence of extra outer membrane layer in *E. coli* as the FE-SEM studies after the treatment of bacteria with CQDs@α-Fe_2O_3 confirmed. Based on the results of the antibacterial activity of α-Fe_2O_3 and CQDs@α-Fe_2O_3 under dark and the light irradiation conditions, it can be concluded that the preferred mechanism of bactericidal activity of hematite-based thin films is both the penetration of iron cations into the bacteria cell via their membrane and the generation of reactive oxygen species via Fenton reaction. Finally, the stability of the samples was tested and found that they had almost their bactericidal activity for at least three times. So, it is expected that the hematite-based nanomaterials can provide insight into the development of visible-light antimicrobial materials for their potential applications in medical devices.

Acknowledgements

The authors would like to thank Research Council of Alzahra University for financial support. A special thanks go to Dr. Juliusz Warzywoda and Dr. Alireza Banazadeh (Texas Tech University, United States) for HRTEM image analysis of the samples. We are also grateful to Dr. Z. Ziaei for her assistance with antibacterial activity of the samples.

==========

Figure Captions

Fig. 1. FE-SEM images from the surface of Ti/α-Fe_2O_3 (a) and Ti/CQD@α-Fe_2O_3 samples prepared by hydrothermal method under the optimized experimental conditions. HRTEM images of CQD@α-Fe_2O_3 sample (c and d).

Fig. 2. The bactericidal activity of the prepared Ti/α-Fe_2O_3 and Ti/CQD@α-Fe_2O_3 samples against *S. aureus* and *E. coli* bacteria strains under dark conditions. The initial concentrations of bacteria strain (CFU/mL) have been indicated in Table 1.

Fig. 3. Zone of inhibition produced by samples Ti/α-Fe_2O_3 (a,b) and Ti/CQD@α-Fe_2O_3 (c,d) against *E. coli* (a,c) and *S. aureus* (b,d) bacterial strains.

Fig. 4. Antibacterial activity of Ti/α-Fe_2O_3 and Ti/CQD@α-Fe_2O_3 samples against *S. aureus* and *E. coli* bacteria strains under visible light irradiation. The initial concentrations of bacteria strain (CFU/mL) have been indicated in Table 1.

Fig. 5. The *E. coli* and *S. aureus* bacteria inactivation kinetics (with an initial concentration of 1.5×10^6 CFU/mL, pH 7.0) by Ti/CQD@α-Fe_2O_3 sample under visible light irradiation.

Fig. 6. The FE-SEM images of native *E. coli* (a) and *S. aureus* (b) and treated *E. coli* (c) and *S. aureus* (d) with Ti/CQD@α-Fe_2O_3 sample under visible light illumination conditions.

==========

Fig. 1

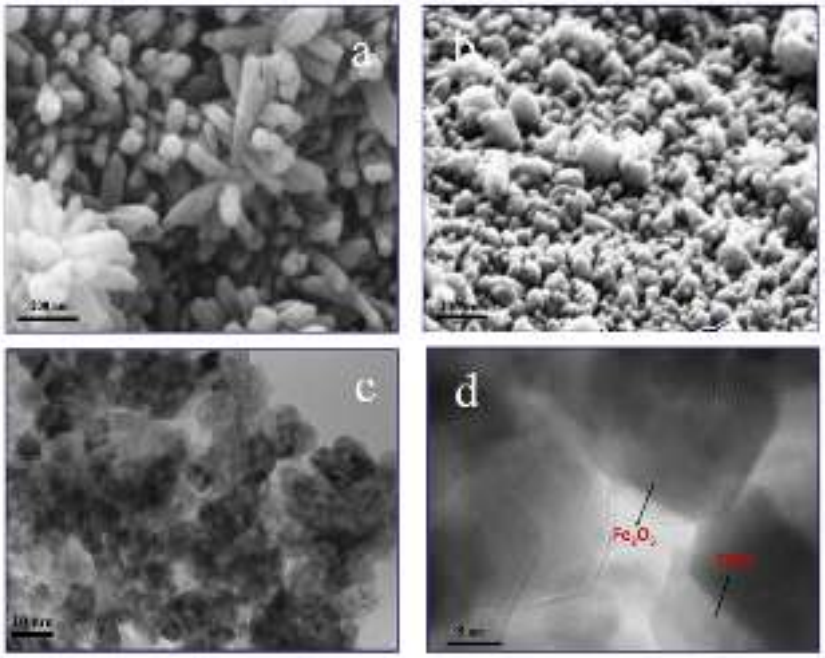

Fig. 2

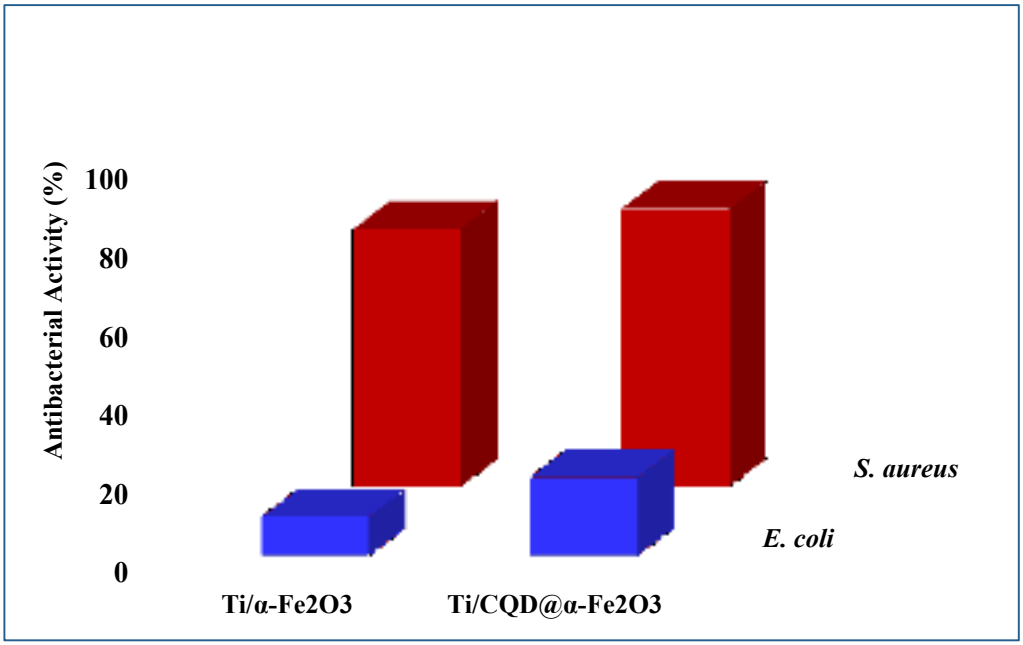
Antibacterial Activity (%)
100
80
60
40
20
0
Ti/α-Fe2O3
Ti/CQD@α-Fe2O3
S. aureus
E. coli

Fig. 3

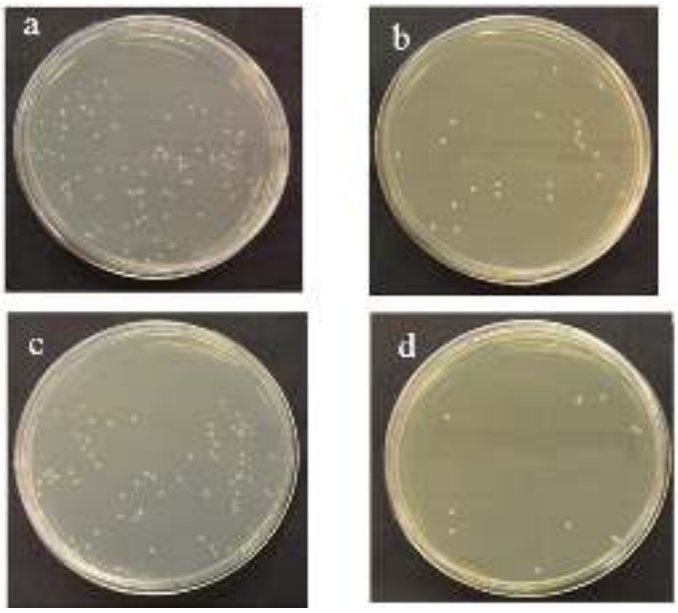
a
b
c
d

Fig. 4

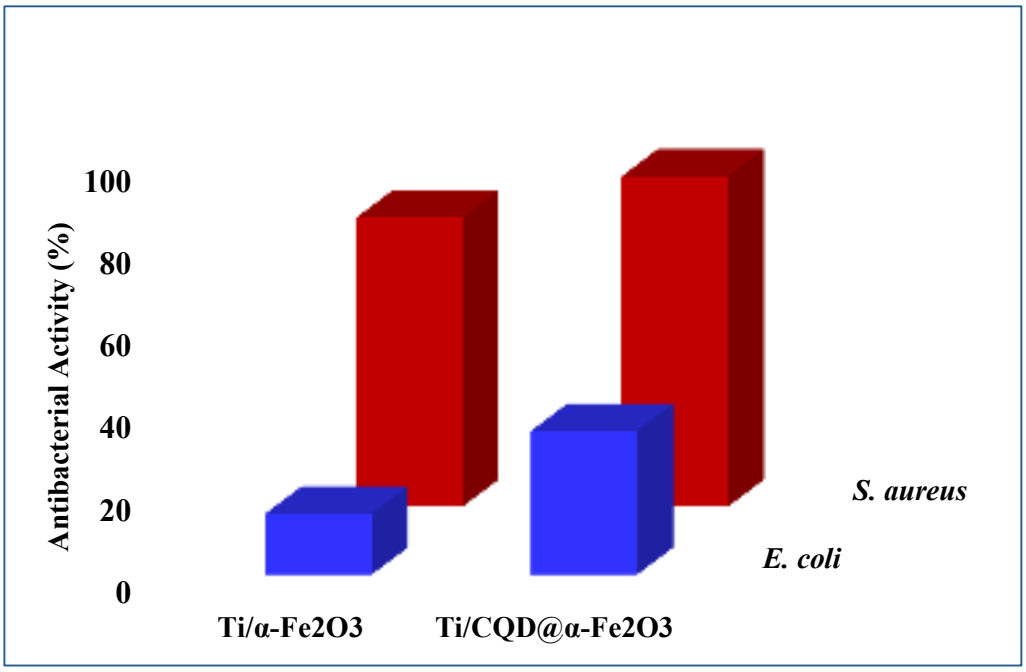
Antibacterial Activity (%)
100
80
60
40
20
0
S. aureus
E. coli
Ti/α-Fe2O3
Ti/CQD@α-Fe2O3

Fig. 5

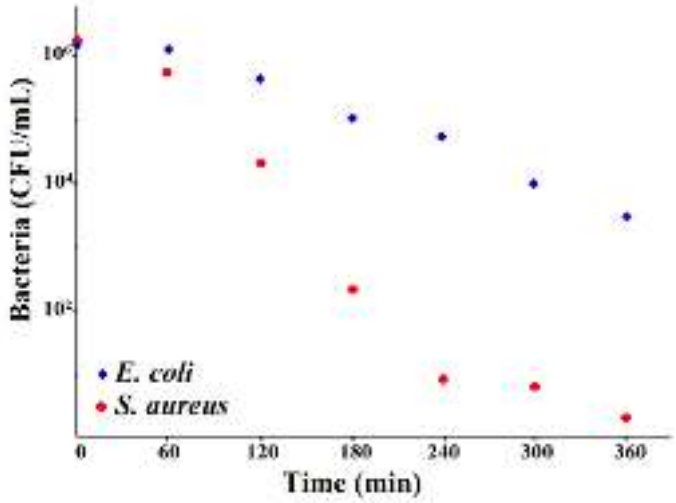
Bacteria (CFU/mL)
E. coli
S. aureus
0
60
120
180
240
300
360
Time (min)

Fig. 6